TARGETING OF POTENTIAL GEOTHERMAL RESOURCES IN THE GREAT BASIN FROM REGIONAL TO BASIN-SCALE RELATIONSHIPS BETWEEN GEODETIC STRAIN AND GEOLOGICAL STRUCTURES

Geoffrey Blewitt[1], Mark F. Coolbaugh[1], Don L. Sawatzky[1],
William Holt[2], James L. Davis[3], and Richard A. Bennett[3]

[1]Great Basin Center for Geothermal Energy, University of Nevada, Reno, NV, USA
[2]State University of New York, Stony Brook, NY, USA
[3]Smithsonian Astrophysical Observatory, Cambridge, MA, USA

Key Words: geothermal, GPS, Great Basin, Nevada, strain, geology, structure, exploration

ABSTRACT

We apply a new method to target potential geothermal resources on the regional scale in the Great Basin by seeking relationships between geologic structures and GPS-geodetic observations of regional tectonic strain. First, we establish a theoretical basis for understanding how the rate of fracture opening can be related to the directional trend of faults within the regional-scale strain field. Second, we develop a strain-structure methodology that uses a digitized database of Quaternary fault strikes and velocities of GPS stations. Results of our strain-structure analysis on the regional scale show a spatial relationship between known geothermal activity and (1) change in the direction of fault orientations, (2) change in the direction of extensional strain, and (3) the magnitude of extensional strain, especially fault-normal extension associated with shear strain. In contrast, the dilitation component of strain is not a significant indicator of geothermal activity in the Great Basin. Using the observed relationships between strain and structure, the NE-SW trending Humboldt structural zone (HSZ) in north-eastern Nevada is clearly identifiable as a regional geothermal target. Based on our detection of an anomalous high in fault-normal extensional strain, we identify Buffalo Valley toward the NE extent of the HSZ as a potential geothermal target to be further explored using GPS. We therefore recommend investigating Buffalo Valley with fine spatial resolution (~10 km rather than the current ~100 km) using a dense GPS network to assess its geothermal potential, by comparison of strain-structure relationships with current power-producing areas within the HSZ.

1. INTRODUCTION

One of the keys to targeting regions with geothermal development potential in the Great Basin is to understand the role of faults in controlling fluid flow in the crust. Prior evidence suggests that critically stressed fractures and faults can play an important role in geothermal fields [Barton et al., 1995; Hickman et al., 1997]. This may be particularly true for geothermal systems in the Great Basin (Figure 1), which unlike most systems in the world are thought not to be magmatic in nature but rather of the type caused by tectonic extension and high heat flow, presumably due to the shallow depth of the Moho [Koenig and McNitt, 1983; Wisian et al., 1999, Blewitt et al., 2003].

The Great Basin Center for Geothermal Energy (GBCGE) is an applied research program of peer-reviewed geothermal research projects with the goal of increasing production and utilization of geothermal energy in the Great Basin. As part of a GBCGE project funded by the U.S. Department of Energy, we test the hypothesis that the continuous regional accumulation of tectonic strain acts

to maintain faults and fractures as conduits for fluid flow, hence acting to sustain geothermal systems. This model would predict an enhancement of this effect if the regional tendency of fault strikes is favorably oriented in the ambient strain field. In particular, maximum effect would be predicted for fault strikes oriented perpendicular to the direction of maximum extensional strain. To test this hypothesis we applied a new method to target potential geothermal resources on the regional scale in the Great Basin by seeking relationships between geologic structures and GPS-geodetic observations of regional tectonic strain. The motivation behind this study is that if the predicted effect were confirmed, it should lead to better regional-scale predictive tools to identify potential targets for geothermal resources. In particular, our strategy is to use regional-scale studies to target future basin-scale investigations, which would then lead to specific localized targets for geothermal exploration, thus connecting blue-sky research to applied engineering.

2. METHODOLOGY

On the regional scale, we investigated the spatial relationship of known geothermal activity with: (1) the regional tendency of Quaternary fault orientations; (2) the direction of extensional strain; and (3) the magnitude of fault-normal extensional strain. Item (1) is purely a structural analysis based on documented Quaternary faulting. Item (2) is purely an empirical strain-rate analysis, based on GPS station velocity data. Item (3) is a combined analysis of both structure and strain-rate. Using observed relationships as a guide, we then infer potential basin-scale targets for future study. We now describe the methodology for each class of analysis.

2.1. STRUCTURE ANALYSIS

A digitized map of Quaternary faults was provided by Craig M. DePolo [pers. comm., 2002], and was integrated into the newly developed GIS at GBCGE [Coolbaugh et al., 2002, 2003], with each fault strike represented as a connected series of line segments. The regional trend in azimuth of faults was computed on a fine grid as a spatial average within circles of 30-km radius. To do this correctly requires the formal application of "directional analysis" and "circular statistics" [e.g., Mardia, 1972]. Fault segments are treated as objects that have an azimuth, but no arrow of direction. The appropriate "average" direction of fault strike can be expressed:

$$\hat{\theta} = \frac{1}{2} \arctan \frac{\langle \sin 2\theta \rangle}{\langle \cos 2\theta \rangle} \qquad (1)$$

where the angle brackets denote the mean value in the usual sense. The "coherence" is defined as

$$\hat{\chi} = \sqrt{\langle \cos 2\theta \rangle^2 + \langle \sin 2\theta \rangle^2} \qquad (2)$$

which must lie between 0 and 1. A coherence of one would be obtained if every line were aligned exactly. A coherence of zero is obtained if for every line there is another line at right angles to it or if the lines were randomly oriented. In the case that the coherence is near zero due to conjugate faulting, the "average azimuth" represents the dominant trend of faults, rather than some azimuth in between. Coherence is a useful statistic for structure-strain analysis (below).

2.2. STRAIN-RATE ANALYSIS

The two-dimensional symmetric strain-rate (velocity gradient) tensor $\mathbf{E}$ can be defined in matrix form:

$$\mathbf{E} = \begin{pmatrix} E_{xx} & E_{xy} \\ E_{yx} & E_{yy} \end{pmatrix}$$

$$= \begin{pmatrix} \dfrac{dv_x}{dx} & \dfrac{1}{2}\left[\dfrac{dv_x}{dy} + \dfrac{dv_y}{dx}\right] \\ \dfrac{1}{2}\left[\dfrac{dv_x}{dy} + \dfrac{dv_y}{dx}\right] & \dfrac{dv_y}{dy} \end{pmatrix} \tag{3}$$

Here the *x*-direction is taken to be eastward, and the *y*-direction northward, and *v* represents velocity. The velocity at a finite number of points is known by time-series analysis of GPS station data, ideally accounting for the effect of seasonal signals [*Blewitt and Lavalleé*, 2002]. The primary GPS velocity data sets used in the Great Basin come from *Wernicke et al.* [2000] and *Thatcher et al.* [1999]. The strain tensor is subsequently computed on a grid by spline interpolation [*Kreemer et al.*, 2000]. The above formula has been simplified here, as the computations are actually done in spherical coordinates to account for Earth curvature.

The strain-rate tensor has four horizontal components at every point on the map. These can be expressed as either cartesian components (as above), or components of rotation (the antisymmetric part) and deformation (the symmetric part). In turn the deformation can be decomposed into one component of dilitation (increase in surface area), and two components of shear (oriented at 45° to each other, the first component of shear corresponding to E-W maximum extension, the second corresponding to NE-SW):

$$D = E_{xx} + E_{yy}$$
$$\gamma_1 = E_{xx} - E_{yy} \tag{4}$$
$$\gamma_2 = 2E_{xy}$$

The magnitude of shear and the direction of shear (direction of maximum extension) is given by:

$$\gamma = \sqrt{\gamma_1{}^2 + \gamma_2{}^2}$$
$$\alpha = \tfrac{1}{2}\arctan\left(\gamma_2/\gamma_1\right) \tag{5}$$

2.3. STRUCTURE-STRAIN ANALYSIS

The rate of extension per unit distance along any azimuth ϕ is given by the tensor dot-product:

$$s(\phi) = \begin{pmatrix} \sin\varphi & \cos\phi \end{pmatrix} \begin{pmatrix} E_{xx} & E_{xy} \\ E_{yx} & E_{yy} \end{pmatrix} \begin{pmatrix} \sin\phi \\ \cos\phi \end{pmatrix}$$
$$= E_{xx}\sin^2\varphi + 2E_{xy}\sin\phi\cos\phi + E_{yy}\cos^2\varphi \tag{6}$$

Blewitt, Coolbaugh, Sawatzky, Holt, Davis, and Bennett

Applying equation (6) to a fault of strike azimuth θ, the extensional strain in the direction normal to the fault $\phi = \theta + 90°$ is given by

$$s_\perp(\theta) = E_{xx}\cos^2\theta - 2E_{xy}\sin\theta\cos\theta + E_{yy}\sin^2\theta \tag{7}$$

Therefore the average extensional strain normal to all fault segments in a region is:

$$\langle s_\perp\rangle = \langle E_{xx}\rangle\langle\cos^2\theta\rangle - \langle E_{xy}\rangle\langle 2\sin\theta\cos\theta\rangle + \langle E_{yy}\rangle\langle\sin^2\theta\rangle \tag{8}$$

where the strain tensor is averaged over the locations of all fault segments in the region. We can use the "average azimuth" and "coherence" from equations (1) and (2) to reconstruct the various geometrical quantities in equation (8):

$$\langle\cos^2\theta\rangle = \tfrac{1}{2}\left(1 + \hat{\chi}\cos 2\hat{\theta}\right)$$
$$\langle\sin^2\theta\rangle = \tfrac{1}{2}\left(1 - \hat{\chi}\cos 2\hat{\theta}\right) \tag{9}$$
$$\langle 2\sin\theta\cos\theta\rangle = \hat{\chi}\sin 2\hat{\theta}$$

Hence equation (8) can be written explicitly in terms of average azimuth and coherence

$$\langle s_\perp\rangle = \frac{\langle E_{xx}\rangle + \langle E_{yy}\rangle}{2} + \hat{\chi}\left[\frac{\langle E_{xx}\rangle - \langle E_{yy}\rangle}{2}\cos 2\hat{\theta} - \langle E_{xy}\rangle\sin 2\hat{\theta}\right] \tag{10}$$

Substituting equation (4) into equation (10) gives:

$$\langle s_\perp\rangle = \frac{1}{2}\left[\langle D\rangle + \hat{\chi}\left(\langle\gamma_1\rangle\cos 2\hat{\theta} - \langle\gamma_2\rangle\sin 2\hat{\theta}\right)\right] \tag{11}$$

Equation (11) tells us something very fundamental. We can get fault-normal extensional strain in one of two ways (or their combination), either (1) by isotropic extension (dilatation), or (2) by a favorable orientation of faults in a shear strain field (such as pull-apart grabens in the step-over of a dominant strike-slip structure). We actually find in the Great Basin that dilitation is relatively small, and the second effect dominates. We can therefore conclude on theoretical grounds that, in the Great Basin, the relative orientation of the shear-strain field with respect to fault strike controls fault-normal extension. By logical inference this shear-strain mechanism most likely controls non-magmatic geothermal systems in the Great Basin.

3. RESULTS

3.1. STRUCTURE RESULTS

The theoretical basis for a possible connection between fault orientation (in the regional strain field) and geothermal activity was established in section 2.3. Figure 2 shows that the NE-SW trending Humboldt structural zone (HSZ) can be characterized as a directional anomaly in the broader regional N-S trend of fault strikes. Note the significant correlation of geothermal activity (Figure 1 and larger circles in Figure 2) with the HSZ. We conclude that the abrupt spatial change in the regional tendency of Quaternary fault orientations is related to geothermal activity in the HSZ.

4

3.2. STRAIN-RATE RESULTS

We also find significant correlation of geothermal activity (Figure 1) with the spatial change in direction of extensional strain-rate as measured by GPS (Figure 3). Note that the trace of geothermal power producing plants distributed along the HSZ, trending NE-SW, falls on a line of abrupt change in the direction of shear when crossing the HSZ in a NW direction. This change in direction of shear might have some correlative cause with the change in azimuth of fault strikes in Fig. 3. One hypothesis that appears to be supported by evidence from seismic surveying is that the crust is thinner along the HSZ than the surrounding region, leading to a change in alignment between the strain and stress fields [Blewitt et al., 2003]. A thinned crust would also explain the trend in location of power producing plants.

3.3. STRUCTURE-STRAIN RESULTS

The above model (crustal thinning) would predict an anomalous increase in strain along the HSZ. This prediction is confirmed by the observed significant spatial correlation of geothermal activity (Figure 1) with the magnitude of fault-normal extensional strain as inferred by both GPS and digitized Quaternary fault maps (Figure 4). There is an increase in the magnitude of this style of strain rate along the Humboldt structural zone trending NE-SW, correlating with the trend of geothermal power plants. Note also the NW-SE trending fault-normal extensional strain along the Walker Lane. Thus the approximate "X" shape pattern approximates the pattern of geothermal temperatures show in Figure 1.

Buffalo Valley is indicated as a local high in fault-normal extensional strain, and thus is identified as a potential target for geothermal exploitation (anomaly in Figure 4.). The stars in Figure 5 at the southern end of Buffalo valley indicate ~1 Ma cinder cones, which may be associated with crustal extension and thinning. Crustal thinning in Buffalo Valley is also indicated by smaller depths to Moho in the seismic data of the GBCGE [Louie, 2002; Blewitt et al., 2003].

4. CONCLUSIONS

We find spatial relationships between geothermal activity in the Great Basin with (1) change in the direction of fault orientations as inferred by digitized Quaternary fault data analysis, (2) change in the direction of extensional strain as inferred by GPS data analysis, and (3) the magnitude of extensional strain, especially fault-normal extension associated with shear strain, as inferred by both GPS and fault analysis. In the Great Basin we find that the relative orientation of the shear strain tensor with respect to fault orientation more likely controls geothermal activity than the dilitation component of strain. By these various considerations, the NE-SW trending Humboldt structural zone (HSZ) in north-eastern Nevada is clearly distinguished as a regional geothermal target. Based on a detection of an anomalous high in fault-normal extensional strain, we identify Buffalo Valley toward the NE extent of the HSZ as a potential geothermal target to be further explored using GPS. We recommend that Buffalo Valley be investigated with fine spatial resolution (~10 km rather than the current ~100 km) using a dense GPS network to assess its geothermal potential. Interpretation of the results could be facilitated by conducting a similar GPS strain-structure analysis in currently exploited areas within the HSZ, such as the Desert Peak-Brady's Hot Springs area.

Blewitt, Coolbaugh, Sawatzky, Holt, Davis, and Bennett

REFERENCES

Barton, C.A., M.D. Zoback, and D. Moos, 1995. Fluid flow along potentially active faults in crystalline rock: Geology, v. 23, p. 683-686.

Blewitt, G., J. Louie, M. Coolbaugh, D. Sawatzky, W. Holt, J. Davis, R. Bennett, and W. Thelen, 2003, Potential for Geothermal Exploration using EarthScope Seismic and GPS Data, *Abstracts of the Joint IRIS-UNAVCO Workshop*, June 19-21, Yosemite.

Blewitt, G., and D. Lavallée, Effect of annual signals on geodetic velocity, *Journ. Geophys. Res., Vol. 107*(B7), 10.1029/2001JB000570, 2002.

Coolbaugh, M.F., Taranik, J.V., Raines, G.L., Shevenell, L.A., Sawatzky, D.L., Minor, T.B., and Bedell, R., 2002, A geothermal GIS for Nevada: defining regional controls and favorable exploration terrains for extensional geothermal systems; Proceedings, Annual GRC Meeting, Reno, NV., Sept. 22-25, 2002, Geothermal Resources Council Transactions, v. 26, p. 485-490.

Coolbaugh, M.F., D.L. Sawatsky, G.L. Oppliger, T.B. Minor, G.L. Raines, L.A. Shevenell, G. Blewitt, and J.N. Louie, 2003, Geothermal GIS coverage of the Great Basin, USA: Defining regional controls and favorable exploration terrains, Proceedings, Annual GRC Meeting, Morelia, Mexico, Oct. 12-15, 2003, Geothermal Resources Council Transactions (this volume).

DePolo, C., Pers. Comm., 2002, Nevada Bureau of Mines and Geology.

Hickman, S., C.A. Barton, M.D. Zoback, R. Morin, J. Sass, and R. Benoit, 1997, In situ stress and fracture permeability along the Stillwater fault zone, Dixie Valley, Nevada: International Jour. of Rock Mechanics and Mining Science, v. 34, p. 414.

Koenig, J.B. and McNitt, J.R., 1983, Controls on the location and intensity of magmatic and non-magmatic geothermal systems in the Basin and Range province; Geothermal Resources Council Special Report No. 13, p. 93.

Kreemer, C., J. Haines, W.E. Holt, G. Blewitt, and D. Lavallée, 2000, On the determination of a global strain rate model, Earth, Planets and Space, 52, 765-770.

Louie, J.N., 2002, Assembly of a crustal seismic velocity database for the Western Great Basin, Transactions Geothermal Resources Council, Vol. 26, (presented at the GRC Meeting, Reno, NV, Sept. 2002).

Mardia, 1972, K.V., Statistics of Directional Data, Academic Press, New York.

Thatcher, W., G.R. Foulger, B.R. Julian, J. Svarc, E. Quilty, and G.W. Bawden, 1999, Present day deformation across the Basin and Range province, western United States: Science, v. 283, p. 1714-1718.

Wernicke, B., A.M. Friedrich, N.A. Niemi, R.A. Bennett, and J.L. Davis, 2000, Dynamics of plate boundary fault systems from Basin and Range geodetic network (BARGEN) and geologic data: GSA Today, v. 10, no.11, p. 1-7.

Wisian, K.W., Blackwell, D.D., and Richards, M., 1999, Heat flow in the western United States and extensional geothermal systems: Proceedings, 24th Workshop on Geothermal Reservoir Engineering, Stanford, CA., p. 219-226.
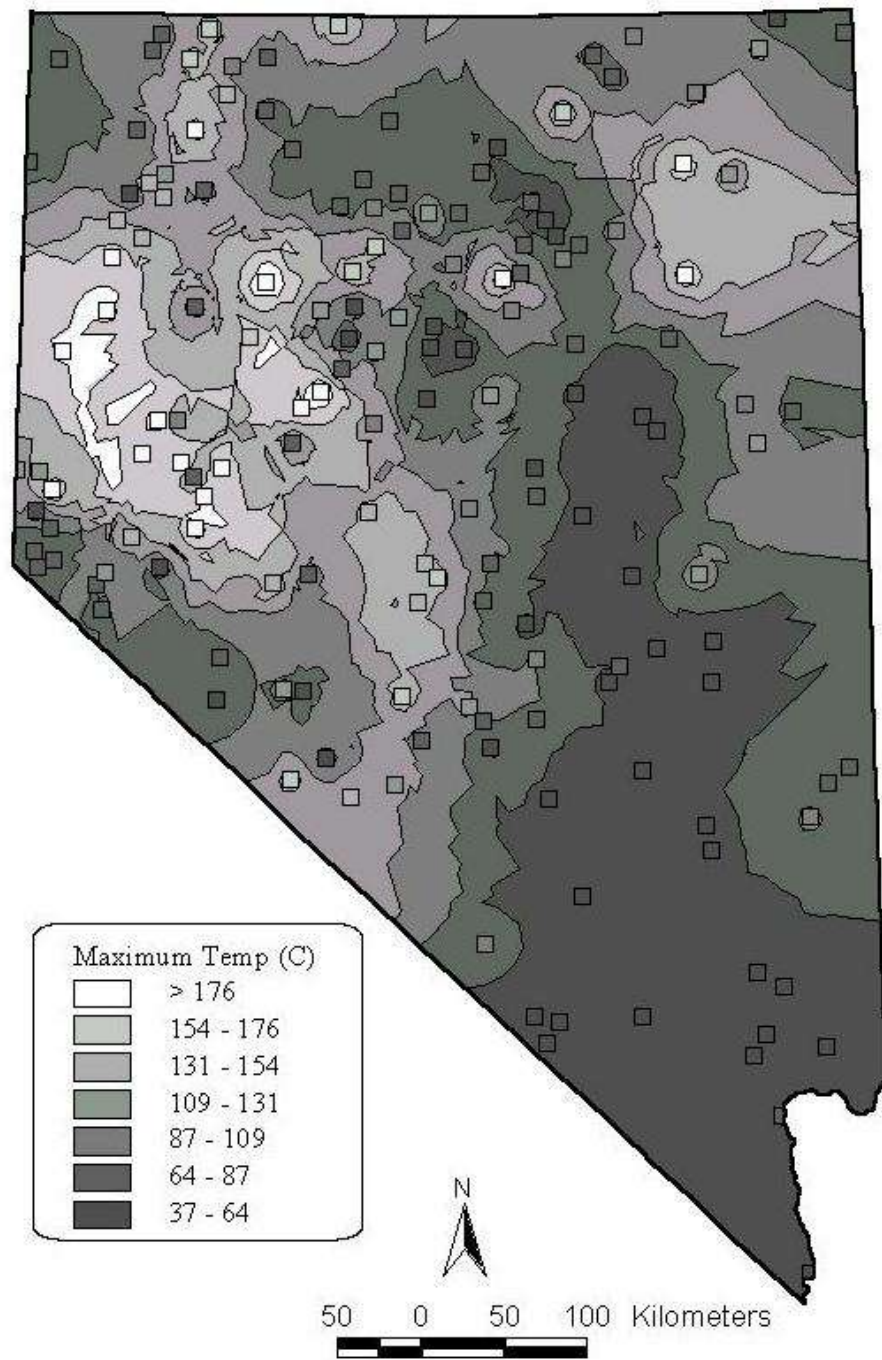
Figure 1. Trend surface of maximum geothermal temperatures. Locations of geothermal systems used for contouring are shown with squares.
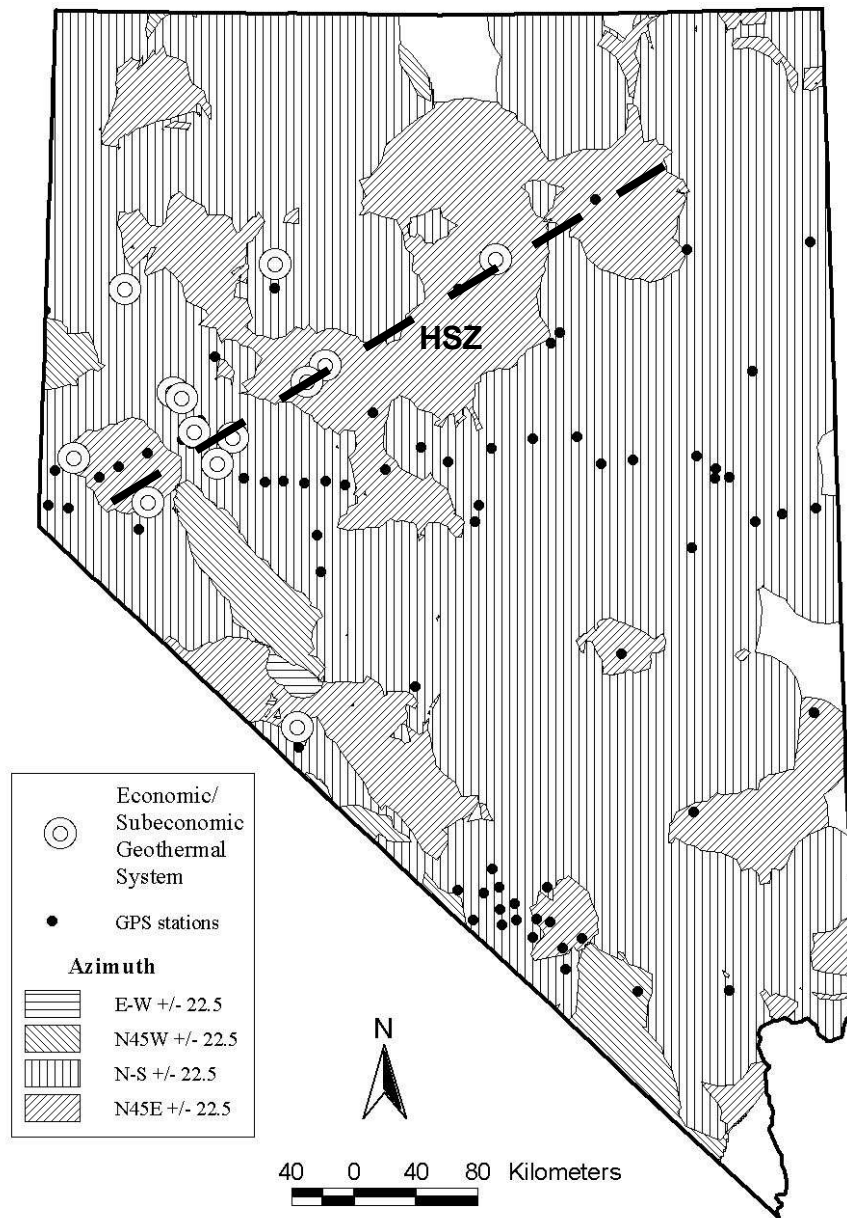
Figure 2: Azimuth map of regionally-averaged Quaternary fault strikes based on rigorous statistical analysis using equation (1), then categorized by fault-trending quadrants. Dots show the location of GPS stations, and larger circles show geothermal power plants. The HSZ appears as NE-SW trending zone (dashed line) of NE-SW trending faults within a sea of predominantly N-S trending faults.
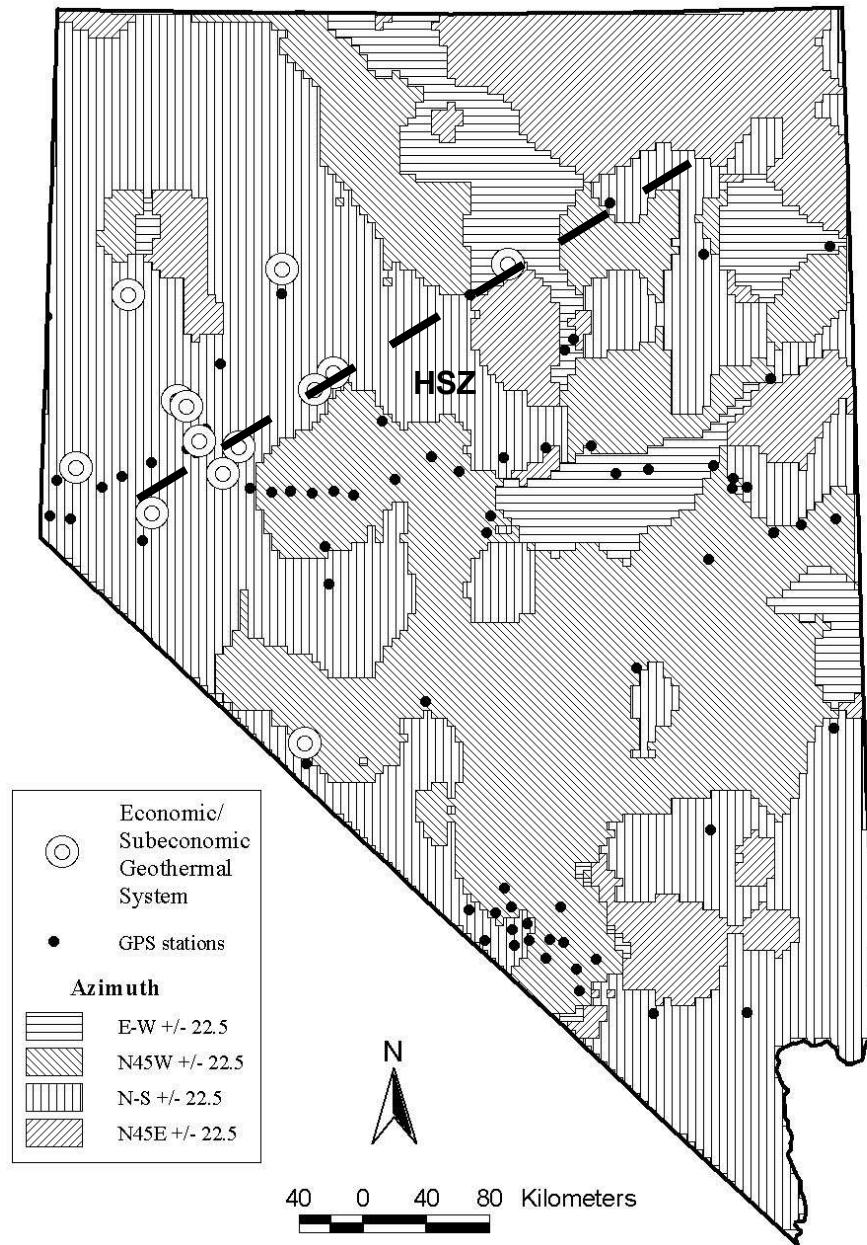
Figure 3: Azimuth map of the direction of regionally-averaged shear strain rates as determined entirely by GPS station velocity data. Geothermal power appears at the eastern end of the HSZ which tends to bisect regions of NW-SE trending shear (to the south) from N-S trending shear (to the north).
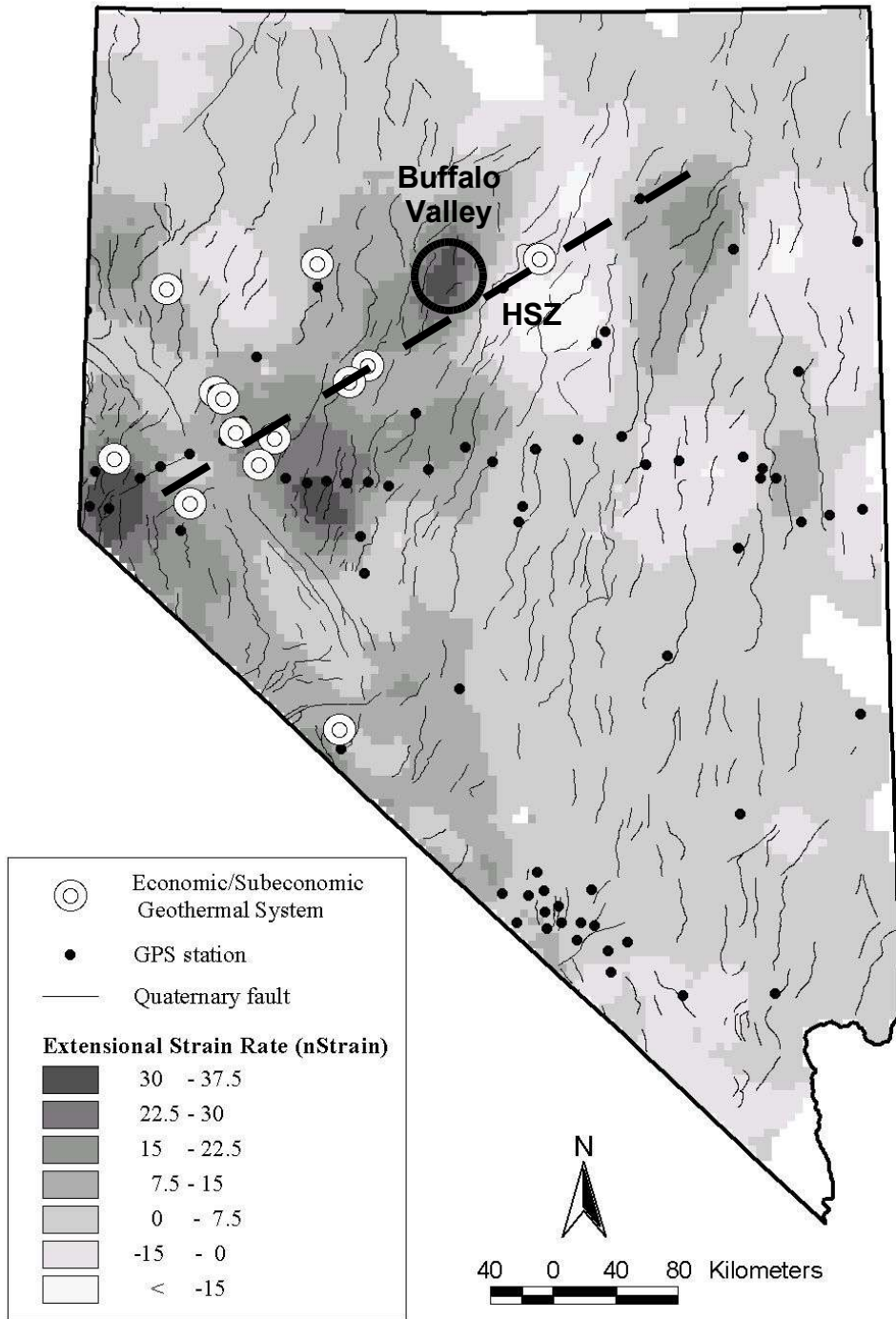
Figure 4: Strain rate map derived from GPS velocities. Specifically, this is the rate of extension normal to the regionally-averaged Quaternary fault strike. The HSZ is delineated particularly in the eastern end by high fault-normal extensional strain. There is significant correlation between this strain map and geothermal temperatures shown in Figure 1. Buffalo Valley, indicated by a circle, shows an anomalously high strain rate.
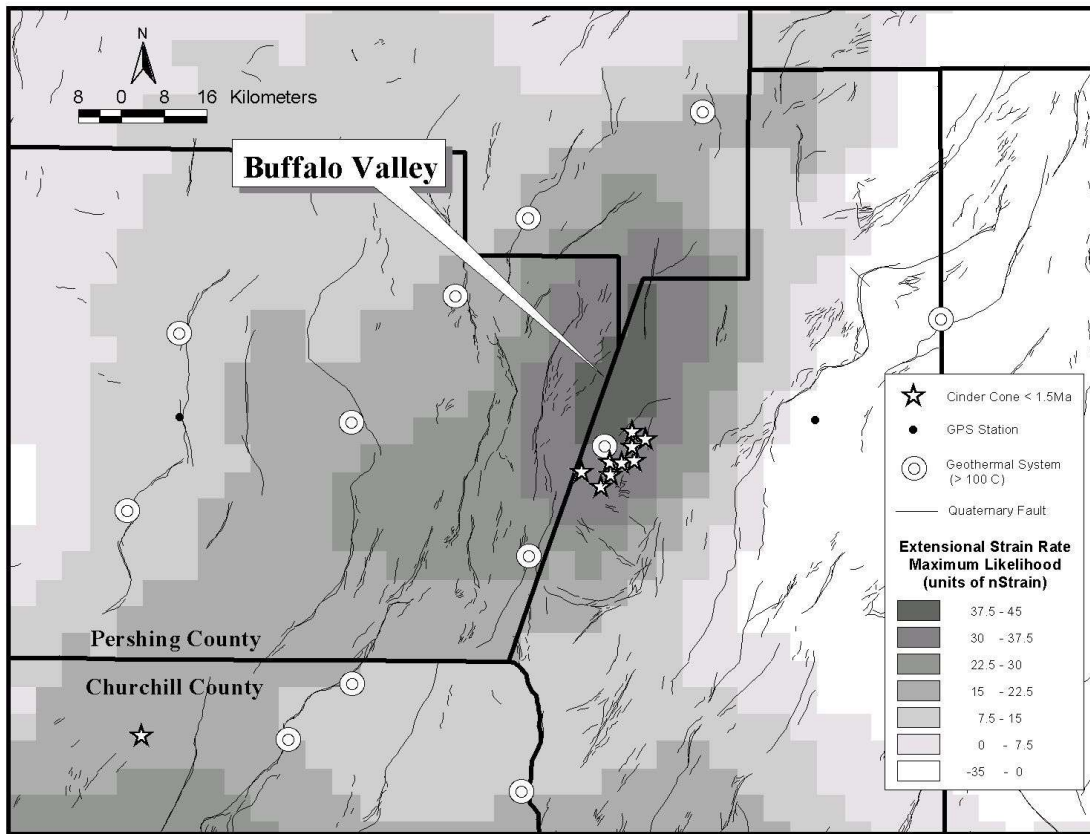
Figure 5: Regional-scale strain-rate map zoomed in on Buffalo Valley. Background shading relates to the magnitude of extensive strain rates perpendicular to fault strike. Stars are ~1 Ma cinder cones.